Optimal Bidding for a Large Battery-Electrolyzer Facility in the Day-ahead Market

Petra Miljan
University of Zagreb (UniZg)
Faculty of Electrical Engineering and Computing (FER)
Zagreb, Croatia
petra.miljan@fer.hr

Zeljko Tomsic
UniZg
FER
Zagreb, Croatia
zeljko.tomsic@fer.hr

Hrvoje Pandzic
UniZg
FER
Zagreb, Croatia
hrvoje.pandzic@fer.hr

***Abstract*—An increasing renewable energy sources (RES) penetration in the recent years has also increased the need for additional flexibility sources and technologies that increase the RES utilization. In addition to battery energy storage, electrolyzers, a technology that produces hydrogen without emitting CO_2, are also receiving an increasing attention. This paper proposes a bi-level profit maximization model for a large battery-electrolyzer facility operation in the day-ahead electricity market. The upper level maximizes the overall profit of the facility, while the lower level simulates the market clearing by maximizing the social welfare. The proposed model is tested on the IEEE RTS-24 test system expanded with wind farms to replicate a modern power system. The presented case study shows how different levels of installed power capacity affect the obtained profit and discusses the battery and electrolyzer utilization.**

***Index Terms*—bi-level optimization, battery, electrolyzer, market clearing**

NOMENCLATURE

Sets and Indices

Ω^b	Set of generator offering blocks
Ω^i	Set of generators
Ω^j	Set of breakpoints in linearized battery charging curve
Ω^k	Set of dual inequality variables
Ω^l	Set of lines
Ω^s	Set of buses
Ω^t	Set of time periods
Ω^w	Set of wind farms

Parameters

α	Variable electrolyzer inefficiency coefficient
β	Fixed electrolyzer inefficiency coefficient
ΔT	Time period (h)
η	Battery roundtrip efficiency
η^{w}	Coefficient of water-to-hydrogen conversion (m^3/kg)
γ^{h}	Coefficient of power-to-hydrogen conversion
κ^{h}	Technical minimum of the electrolyzer (%)
$\lambda^{\mathrm{g}_{i,b}}$	Price bid of block *b* generator *i* (€/MWh)
λ^{h}	Hydrogen price (€/kg)
λ^{w}	Cost of water (€/m^3)
$D_{t,s}$	Power demand at bus *s* at time *t* (MW)
$\overline{F_l}$	Maximum power flow through line *l* (MW)
$F_{l,s}^{\mathrm{map}}$	Line–bus incidence matrix
F_j	Coefficients for charging curve linearization
$\overline{G_{i,b}}$	Maximum power output of production block *b* of generator *i* (MWh)
$G_{i,s}^{\mathrm{map}}$	Generator–bus incidence matrix
M	Large positive number
P^{ch}	Maximum battery power rating (MW)
P^{ekz}	Maximum power of the electrolyzer (MW)
R_j	Coefficients for charging curve linearization
RD_i/RU_i	Ramp down / up limit for each generator *i* (MWh)
$\overline{soe}$	Maximum battery capacity (MWh)
$\overline{W_{t,w}}$	Maximum power output of wind farm *w* at time *t* (MWh)
$W_{w,s}^{\mathrm{map}}$	Wind farm–bus incidence matrix
Y_l	Susceptance of line *l* (μS)

Variables

χ_t^{h}	Produced hydrogen amount (kg)
$\lambda^{\mathrm{b}}/\lambda^{\mathrm{s}}$	Price of purchased/sold electricity
Π^{e}	Profit from electricity trading (€)
Π^{h}	Profit from hydrogen trading (€)
$\vartheta_{t,s}$	Angle at bus s at time *t* (rad)
ζ^{w}	Water consumption costs (€)
b_t^{bat}	Binary variable, 1 if baterry is charging 0 otherwise
b_t^{h}	Binary variable, 1 if electrolyzer is on 0 otherwise
$f_{t,l}$	Power flow through line *l* at time *t* (MW)
$g_{t,i,b}$	Output power of block *b* generator *i* at time *t* (MW)
p_t^{h}	Actual power required to produce a kilogram of hydrogen at time *t* (MW)
$\overline{p_t^{\mathrm{ch}}}/\overline{p_t^{\mathrm{dis}}}$	Battery charging/discharging quantity bid at time *t* (MW)
$\overline{p_t^{\mathrm{h}}}$	Electrolyzer power consumption at time *t* (MW)
$p_t^{\mathrm{ch}}/p_t^{\mathrm{dis}}$	Baterry charging/discharging powerat time *t* (MW)
p_t^{h}	Power consumption of the electorlyzer at time *t* (MW)
$soe_{t,j}$	State of energy at the segment *j* (MWh)
soe_t	Battery state of energy at time *t* (MWh)
$w_{t,w}^{\mathrm{prod}}$	Ouput power of wind farm *w* at time *t* (MW)

This work was partially funded by the European Union through the European Regional Development Fund Operational Programme Competitiveness and Cohesion 2014-2020 of the Republic of Croatia under project KK.01.1.1.04.0034 "Connected Stationary Battery Energy Storage". This work was also supported in part by the Croatian Science Foundation and European Union through the European Social Fund under the project Flexibility of Converter-based Microgrids – FLEXIBASE (PZS-2019-02-7747).

I. Introduction

Over the past decades, due to the high penetration of renewable energy sources (RES) and their operational intermittency, the system's need for solutions that provide additional flexibility has increased. Some of the already established alternatives for providing additional flexibility to the system and better RES utilization are the energy storage integration [1] and the end-users activation [2]. However, the most recent alternative solutions to the flexibility challenge is green hydrogen (GH). It is hydrogen produced from RES electricity via electrolysers, which makes it the only zero-carbon way of hydrogen production [3].

EU plans on installing at least 6 GW of electrolyzers by 2024 and 40 GW by 2030, while the analysts estimate that GH could meet 24% of the world energy demand by 2050 [4]. On the other hand, it will take approximately 6-10 years to build up both the needed infrastructure and prepare the market [5]. To address the profit maximization problem of the future large-scale electrolyzers, this paper develops a bi-level strategic bidding model that maximizes the profit from the day-ahead market arbitrage performed by a facility consisting of an electrolyzer and a battery in the upper level, while the lower level maximizes the social welfare. The proposed model is used to investigate the market behavior of such independent strategic market player.

A. Literature Review

Bi-level optimization is a mathematical tool that can be used for modeling of price-making agents in the market. Typically, the decision-maker from the upper-level problem participates in the lower-level problem common to all market participants. The strategic player assumes the other players bid and their marginal costs and consider their bids as parameters, i.e. the other players are not strategic. Bi-level models are commonly used in the liberalized electricity market environment where many players have conflicting objectives.

Paper [6] considers a battery operation in the day-ahead electricity market, owned and operated by an independent entity. Paper [7] models an aggregated battery swapping stations (BSS) as a strategic market player. Both of the referenced bi-level models, consisting of the profit maximization upper-level problem and electricity market clearing in lower-level, are first reduced to a single-level problem by the Karusch-Kuhn-Tucker (KKT) transformation. Afterward, the developed model is used to analyze the roles and opportunities of batteries/BSS as active participants in the electricity market. Since batteries can participate not only in the energy market but also in the reserves market, [8] proposes a bilevel model for the interaction of different markets, e.g. day-ahead and balancing markets.

The disproportion between the costs of RES and conventional generators can cause price suppression. Paper [9] through a developed bilevel model and an illustrative case study shows how price suppression, caused by high wind penetration, is affected through the integration of energy storage. Energy storage integration brings not only advantages but also disadvantages, so it is essential to investigate what effect do the size, location, charging/discharging rate, and efficiency of energy storage have on electricity prices and transmission line congestion [10]. It is important to bear in mind that most research papers investigate energy storage impact to perfect market conditions. Since perfect conditions are rarely possible in reality, paper [11] considers imperfections in the market.

Even though there are papers considering dependencies between the electricity and the gas markets [12] as well as gas-fired units as market players [13], there are still very few papers dealing with both the hydrogen and the electricity markets. Paper [14] investigates the role of hydrogen to increase the penetration of RES. The proposed bi-level model minimizes the total annual cost of the needed equipment in the upper level, and minimizes the levelized cost of hydrogen supply in the lower level. Paper [15] investigates a long-term investment in a hydrogen system that would utilize the China's high hydropower potential. From the perspective of a distribution system operator aiming to maximize its profit, paper [16] considers the scheduling of a hydrogen-based microgrid. For the hydrogen market to develop, it is crucial to develop an economically and environmentally sustainable hydrogen supply chain, and one such bi-level model is proposed in [17].

In light of the conducted literature review, this paper proposes a bi-level profit maximization model for an operation of a battery-electrolyzer facility in the day-ahead electricity market. The facility is considered a price maker in the electricity market. The advanced model of a battery, which takes into account the dependence between the charging power and the battery's state of energy, is employed. In the electrolyzer modeling, the relationship between the hydrogen production and electricity consumption is linearized. The proposed model is tested on the IEEE RTS-24 test system for different levels of installed capacity of both the battery and the electrolyzer. The existing system, which consists only of conventional generators, has been expanded with nine wind turbines. Wind turbines are connected to the grid by frequency converters. The battery exchanges electricity with the grid through a bidirectional AC-DC converter, while the electrolyzer withdraws electricity from the grid through an AC-DC converter. The realized profits and the utilization of such facility are discussed.

II. Mathematical model

The proposed bi-level model consists of the upper-level problem, which aims to maximize the overall profit, and the lower-level problem, which aims at maximizing the social welfare. The model is based on following assumptions:

- the price of hydrogen is constant throughout time;
- there is a demand for all hydrogen produced regardless of the quantity;
- electricity network constraints are based on the dc approximation;
- the facility is considered a price maker in the electricity market;
- the wind farms bidding price is 0 €/MWh.

A. Upper-Level Problem

The objective function of the upper-level (1) maximizes the difference between the profits from electricity trading (2) and hydrogen trading (3) on one hand, and the cost of consumed water for hydrogen production (4) on the other. Equations (5)–(8) are the electrolyzer constraints, and equations (9)–(18) are the battery constraints. Eqs. (5) and (6) indicate the minimum and maximum electrolyzer's operating power constraints. Eqs. (7) and (8) show the actual relationship between the required power of the electrolyzer and the produced hydrogen. Eq. (7) indicates a relationship between the power of the electrolyzer itself and the produced hydrogen, while eq. (8) calculates the amount of power purchased from the energy market to supply the electrolyzer. Since the electrolyzer's efficiency changes with its operating point, the first part of eq. (8) defines the variable part of the electrolyzer's power consumption, while the second part accounts for the electrolyzer's fixed power consumption when turned on. The advanced battery model, where the charging power depends on the current battery's state of energy (9)–(18) is taken from [18].

$$Max_{p_t^{\mathrm{ch}},p_t^{\mathrm{dis}},\chi_t^{\mathrm{h}}} \Pi^{\mathrm{e}} + \Pi^{\mathrm{h}} - \zeta^{\mathrm{w}} \tag{1}$$

subject to

$$\Pi^{\mathrm{e}} = \sum_t (p_t^{\mathrm{dis}} - p_t^{\mathrm{ch}} - p_t^{\mathrm{h}}) \cdot \Delta T \cdot \lambda_{1,t,s} \tag{2}$$

$$\Pi^{\mathrm{h}} = \sum_t \chi_t^{\mathrm{h}} \cdot \lambda^{\mathrm{h}} \tag{3}$$

$$\zeta^{\mathrm{w}} = \sum_t \chi_t^{\mathrm{h}} \cdot \eta^{\mathrm{w}} \cdot \lambda^{\mathrm{w}} \tag{4}$$

$$p_t^{\mathrm{h}} \leq P^{\mathrm{ekz}} \cdot b_t^{\mathrm{h}}, \ \ \forall t \in \Omega^t \tag{5}$$

$$p_t^{\mathrm{h}} \geq \kappa^{\mathrm{h}} \cdot P^{\mathrm{ekz}} \cdot b_t^{\mathrm{h}}, \ \ \forall t \in \Omega^t \tag{6}$$

$$\hat{p_t^{\mathrm{h}}} = \chi_t^{\mathrm{h}} \cdot \gamma^{\mathrm{h}}, \ \ \forall t \in \Omega^t \tag{7}$$

$$\hat{p_t^{\mathrm{h}}} = \alpha \cdot p_t^{\mathrm{h}} + \beta \cdot P^{\mathrm{ekz}} \cdot b_t^{\mathrm{h}}, \ \ \forall t \in \Omega^t \tag{8}$$

$$soe_t = soe_{t-1} + p_t^{\mathrm{ch}} \cdot \eta \cdot \Delta T - p_t^{\mathrm{dis}} \cdot \Delta T \ \ \forall t \in \Omega^t \setminus 1 \tag{9}$$

$$soe_1 = soe_0 + p_1^{\mathrm{ch}} \cdot \eta \cdot \Delta T - p_1^{\mathrm{dis}} \cdot \Delta T \tag{10}$$

$$soe_t \leq \overline{soe} \ \ \forall t \in \Omega^t \tag{11}$$

$$soe_T \geq soe_0 \tag{12}$$

$$soe_t = \sum_{j=1}^{J-1} soe_{t,j}, \ \ \forall t \in \Omega^t \tag{13}$$

$$soe_{t,j} \leq R_{j+1} - R_j, \ \ \forall j \in \Omega^j, \forall t \in \Omega^t \tag{14}$$

$$\Delta soe_t = F_1 + \sum_{j=1}^{J-1} \frac{F_{j+1} - F_j}{R_{j+1} - R_j}, \ \ \forall t \in \Omega^t \tag{15}$$

$$\overline{p_t^{\mathrm{ch}}} \leq \frac{P^{\mathrm{ch}} \cdot \Delta soe_t}{\eta}, \ \ \forall t \in \Omega^t \tag{16}$$

$$\overline{p_t^{\mathrm{ch}}} \leq b_t^{\mathrm{bat}} \cdot M, \ \ \forall t \in \Omega^t \tag{17}$$

$$\overline{p_t^{\mathrm{dis}}} \leq (1 - b_t^{\mathrm{bat}}) \cdot M, \ \ \forall t \in \Omega^t \tag{18}$$

B. Lower-Level Problem

The objective function (19) of the lower-level problem maximizes the social welfare. Equation (20) is the power balance constraint of the system. Equations (21)–(23) are line flows constraints: eq. (21) calculates the line power flows, eq. (22) sets the reference bus' voltage angle to zero and eq. (23) limits the minimum and maximum line flow. Equations (24) and (27) limits the wind farm and generator outputs. Equations (25) and (26) indicate each generator's ramp-up and ramp-down constraints. Equations (28)–(30) limit the the battery-electrolyzer facility's cleared power quantities so that they do not exceed the bid quantity.

$$\mathrm{Max}(\sum_t (p_t^{\mathrm{ch}} + p_t^{\mathrm{h}}) \cdot \lambda^{\mathrm{b}} - \sum_t p_t^{\mathrm{dis}} \cdot \lambda^{\mathrm{s}} - \sum_{t,i,b} g_{t,i,b} \cdot \lambda^{\mathrm{g}_{i,b}}) \cdot \Delta T \tag{19}$$

subject to

$$\sum_w w_{t,w}^{\mathrm{prod}} \cdot W_{w,s}^{\mathrm{map}} + \sum_{i,b} g_{t,i,b} \cdot G_{i,s}^{\mathrm{map}} \sum_l f_{t,l} \cdot F_{l,s}^{\mathrm{map}} = \\ = D_{t,s} + p_t^{\mathrm{ch}} + p_t^{\mathrm{h}} - p_t^{\mathrm{dis}}, \ \ \forall s \in \Omega^s, \forall t \in \Omega^t : \lambda_{1,t,s} \tag{20}$$

$$f_{t,l} = Y_l \sum_s \vartheta_{t,s} \cdot F_{l,s}^{\mathrm{map}}, \ \ \forall l \in \Omega^l, \forall t \in \Omega^t : \lambda_{2,t,s} \tag{21}$$

$$\vartheta_{t,s} = 0, s = \mathrm{ref.bus}, \forall t \in \Omega^t : \lambda_{3,t,s} \tag{22}$$

$$-\overline{F_l} \leq f_{t,l} \leq \overline{F_l}, \ \ \forall l \in \Omega^l, \forall t \in \Omega^t : \underline{\mu_{1,t,l}}, \overline{\mu_{1,t,l}} \tag{23}$$

$$0 \leq w_{t,w}^{\mathrm{prod}} \leq \overline{W_{t,w}}, \ \ \forall w \in \Omega^w, \forall t \in \Omega^t : \underline{\mu_{2,t,w}}, \overline{\mu_{2,t,w}} \tag{24}$$

$$\sum_b (g_{t,i,b} - g_{t-1,i,b}) \leq RU_i, \ \ \forall i \in \Omega^i, \forall t \in \Omega^t : \mu_{3,t,i} \tag{25}$$

$$\sum_b (g_{t-1,i,b} - g_{t,i,b}) \leq RD_i, \ \ \forall i \in \Omega^i, \forall t \in \Omega^t : \mu_{4,t,i} \tag{26}$$

$$0 \leq g_{t,i,b} \leq \overline{G_{i,b}}, \ \ \forall i \in \Omega^i, \forall b \in \Omega^b, \forall t \in \Omega^t : \underline{\mu_{5,t,i,b}}, \overline{\mu_{5,t,i,b}} \tag{27}$$

$$0 \leq p_t^{\mathrm{ch}} \leq \overline{p_t^{\mathrm{ch}}}, \ \ \forall t \in \Omega^t : \underline{\mu_{6,t}}, \overline{\mu_{6,t}} \tag{28}$$

$$0 \leq p_t^{\mathrm{dis}} \leq \overline{p_t^{\mathrm{dis}}}, \ \ \forall t \in \Omega^t : \underline{\mu_{7,t}}, \overline{\mu_{7,t}} \tag{29}$$

$$0 \leq p_t^{\mathrm{h}} \leq \overline{p_t^{\mathrm{h}}}, \ \ \forall t \in \Omega^t : \underline{\mu_{8,t}}, \overline{\mu_{8,t}} \tag{30}$$

C. Transformation to MPEC

Due to its bi-level structure, commercial solvers cannot solve the given problem. Instead, it has to be transformed into a mathematical program with equilibrium constraints (MPEC). One way to achieve this is to replace the lower-level with its KKT conditions. A more interested reader can find used KKT conditions for a given problem in the Appendix. Dual variables of the lower-level constraints above are listed after a colon. The final linearized objective function is given in eq. (31) .

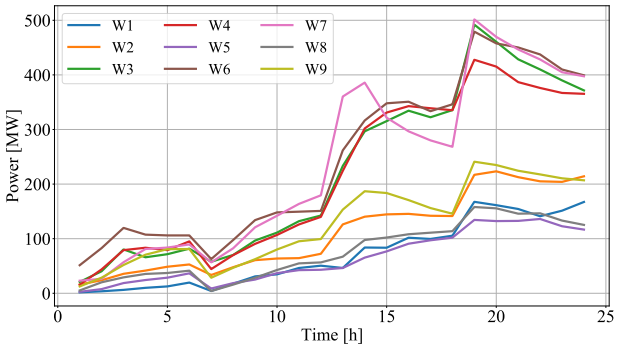

Fig. 1. Output power of wind farms

$$\text{Max} -\sum_{t,i,b} g_{t,i,b}\cdot\lambda^{g_{i,b}}\cdot\Delta T+\sum_{s,t} D_{t,s}\cdot\lambda_{1,t,s}-\sum_{i,t} RU_i\cdot\mu_{3,t,i} -\sum_{i,t} RD_i\cdot\mu_{4,t,i}-\sum_{l,t}\overline{F_l}\cdot\overline{\mu_{1,t,l}}-\sum_{w,t}\overline{W_{t,w}}\cdot\overline{\mu_{2,t,w}} -\sum_{l,t}\overline{F_l}\cdot\underline{\mu_{1,t,l}}-\sum_{t,i,b}\overline{G_{i,b}}\cdot\overline{\mu_{5,t,i,b}}+\Pi^{\text{h}}-\zeta^{\text{w}} \quad (31)$$

III. Case Study

To obtain the conditions of a modern power system to demonstrate the proposed model, we used the IEEE RTS-24 expanded with nine wind farms from [19]. The wind output throughout the day is provided in Figure 1. However, to match the price levels obtained in the current electricity markets, the generator-offered prices were multiplied by a factor of three.

The problem is modeled in GAMS and solved for one day with a time step of one hour using the Gurobi 9.1.2 solver. A computational time of the model, run on the 11th Gen Intel(R) Core(TM) i7-1165G7 with 16 GB of RAM, is 1,8 s. The model has 31709 constraints and 23020 variables.

The facility's offering and bidding prices are set to 0 €/MW and 100 €/MW, respectively. The battery roundtrip efficiency is set to 0,9 and the initial state of energy is set to 50%. Prices of hydrogen and water are set to 1 €/kg and 0.397 €/m^3, respectively. The coefficient of water-to-hydrogen conversion is set to 0,01, electrolyzers technical minimum is set to 10% while coefficients γ^{h}, α and β are set to 0,0394, 0,689 and 0,011 respectively [20]. Four different cases with different installed battery and electrolyzer capacities are considered. The battery and the electrolyzer's installed capacity were set to 20 MW, 50 MW, 100 MW, and 200 MW in the simulations. The battery net energy rating is equal to its power capacity, meaning it can fully discharge within an hour. However, since the model uses an accurate battery model from [18], it cannot fully charge within one hour.

Figure 2 shows locational marginal prices (LMP) at each bus. When we compare the wind production (shown in Figure 1) with LMPs, it is important to note that LMPs drastically decrease during periods of high wind production, even turning negative at some buses.

Table I shows how the profit increases depending on the increasing capacity. The increase of the installed capacity, however, diminishes the marginal realized profit. Even though the installed capacity increases 2,5 times, in the case of 50 MW versus 20 MW, the realized profit increases only 2,35 times. For 100 MW installed capacity the realized profit increases 1,74 times as compared to the 50 MW capacity. The biggest difference, however, is visible between the last two cases (100 vs. 200 MW), where a double increase in the installed capacity results in only 1,4 times higher profit. This trend is also confirmed by the last row of Table I showing how profits per MW decrease with the increasing installed capacity.

TABLE I
Total profit per case and profit per MW of installed power

Capacity	**20 MW**	**50 MW**	**100 MW**	**200 MW**
Profit	5.252,85 €	12.367,57 €	21.476,85 €	30.120,07 €
Profit per MW	262,64 €	247,35 €	214,77 €	150,60 €

Figures 3-6 show how the battery is charged/discharged and how much power the electrolyzer consumes depending on the price signals during the day for different installed capacities when the facility is located at bus 3.

Figure 3 shows the the results for 20 MW installed capacity. In this case, the electrolyzer maximizes utilization of its capacity during the low-price periods in the second half of the day. The electrolyzer does not consume maximum power in hour 14 because it would increase the LMP, which would increase the purchasing cost of hydrogen, resulting in lower overall profit. The same is confirmed by Figure 7, which shows the production of hydrogen per hour for the four installed capacities. From hour 15 until the end of the day the electrolyzer constantly produces 349,75 kg of hydrogen per hour. In parallel to the electrolyzer operation, the battery performs arbitrage by charging at the low-price periods and discharging during high-price periods. It performs three full cycles during the day, taking advantage of negative prices in the second half of the day. Since we are using the accurate battery charging model that considers the lower charging ability at higher states of charge, the battery cannot charge within one hour, but commonly uses a subsequent hour to top up.

For 50 MW installed capacity the results are shown in

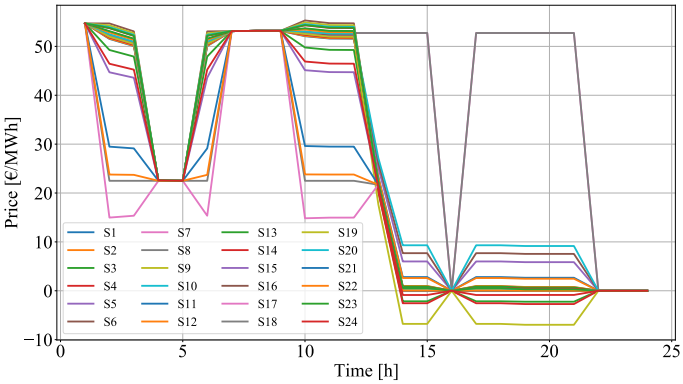

Fig. 2. LMP at each bus

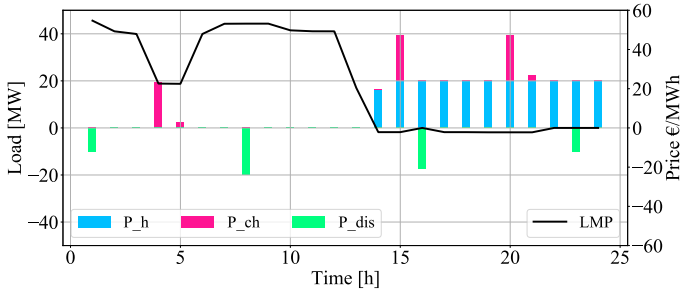

Fig. 3. Charging and discharging power of the battery, consumption of the electrolyzer, and LMPs at bus 3 for 20 MW installed capacity

Figure 4. The electrolyzer also operates at maximum power in hours 15-24. However, in this case in hour 14 the electrolyzer works with power significantly lower than the maximum not to affect the LMP. This is also shown in Figure 7 where the slope between the non-production and the maximum production is much steeper. The maximum hydrogen production in this case is 874,37 kg per hour. The battery charges in hours 4-5, 16, and 19-21, and discharges in hours 1, 3, 8-9, 18, 22, and 24. The maximum charging power in this case, is 48,22 MW which is almost its full charging potential. The maximum discharging power in this case is 27,32 MW, which is slightly more than half of the full discharging potential. In this case, the overall facility draws the maximum power only in hour 19.

Figure 5 shows the case with installed capacity 100 MW. In this case, the electrolyzer operates in hours 14-24, as in both previous cases. But unlike the previous cases, the electrolyzer's production is not so uniform. It operates at full capacity in hours 16 and 19-24, but in other hours it works at 15-80% of full capacity not to increase the LMPs. The maximum produced hydrogen in one hour is 1748,73 kg. Unlike the electrolyzer, the battery does not utilize its full capacity at any time period, meaning that the 100 MW capacity is overdimensioned for this location and network conditions. The maximum charging power is 47,58 MW and it occurs in hour 5. The maximum discharging power 51,64 MW occurs in hour 8. This means that only 50% of the full battery charging/discharging potential is utilized.

The results of the final case with the maximum installed capacities is shown in Figure 6. In this case, the electrolyzer operates at its full capacity only in hours 23 and 24, while in other hours it utilizes 40-75% of its full capacity. Figure 7 also confirms this as it exhibits the largest oscillations in hydrogen production. The maximum production of hydrogen in one hour is 3497,46 kg. The battery charges in hours 4-5, 16, and 23-24, and discharges in hours 1 and 8-9. The maximum charging power is 81,40 MW, i.e. 40% of the charging potential. The maximum discharging power is 100 MW. The largest exchange between the network and the facility takes place in hour 24 and amounts to 70% of the total installed capacity of the facility.

IV. Conclusion

A model for the large battery-electrolyzer facility participation in the day-ahead market is proposed. Looking at the case study, several conclusions can be drawn. First, the penetration

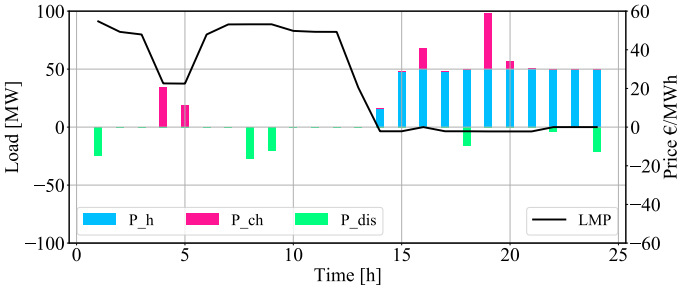

Fig. 4. Charging and discharging power of the battery, consumption of the electrolyzer, and LMPs at bus 3 for 50 MW installed capacity

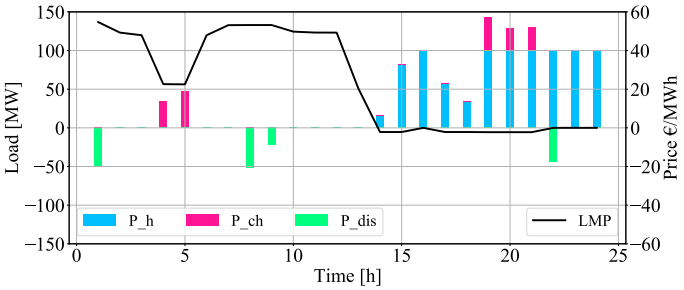

Fig. 5. Charging and discharging power of the battery, consumption of the electrolyzer, and LMPs at bus 3 for 100 MW installed capacity

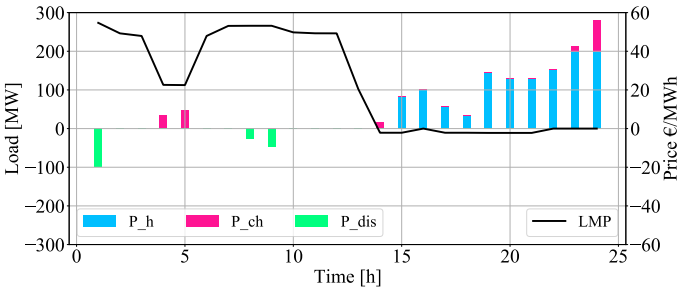

Fig. 6. Charging and discharging power of the battery, consumption of the electrolyzer, and LMPs at bus 3 for 200 MW installed capacity

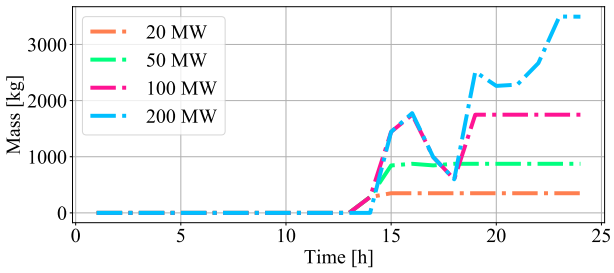

Fig. 7. Mass of produced hydrogen per installed capacity

of RES, or in this case wind farms, significantly affects the LMPs, whose values can be exploited in different ways. While the battery energy storage exercises arbitrage taking advantage of price differences (the absolute price values are not as important), the electrolyzer finds attractive only the lowest prices. Finally, even at favorable prices, the facility avoids operating at full capacity in cases it would increase the LMP and, consequently, reduce the overall profit.

Since batteries and electrolyzers are expensive technologies,

the conducted case study demonstrates the importance of appropriate sizing of such facility, which is a research line left for future work. Additionally, it is important to assess the ratio of the electrolyzer's and the battery's capacity to maximize the return on investment.

Overall, the large battery-electrolyzer facility increases the RES utilization while achieving profit. With the increasing development of hydrogen infrastructure and the increasing use of batteries, such facilities are expected to come to life.

APPENDIX

$$-\sum_s G^{\text{map}}_{i,s}\cdot\lambda_{1,t,s}+\lambda^{\text{g,i,b}}+\mu_{3,t,i}-mu_{3,t+1,i}-\mu_{4,t,i}+\mu_{4,t+1,i} +\overline{\mu_{5,t,i,b}}-\underline{\mu_{5,t,i,b}}=0,\ \ \forall t\in\Omega^t,\forall i\in\Omega^i,\forall b\in\Omega^b \quad (32)$$

$$\sum_s\lambda_{1,t,s}+\overline{\mu_{6,t}}-\underline{\mu_{6,t}}-\lambda^{\text{b}}=0,\quad s=\text{ref.bus},\forall t\in\Omega^t \quad (33)$$

$$-\sum_s\lambda_{1,t,s}+\overline{\mu_{7,t}}-\underline{\mu_{7,t}}+\lambda^{\text{s}}=0,\quad s=\text{ref.bus},\forall t\in\Omega^t \quad (34)$$

$$\sum_s\lambda_{1,t,s}+\overline{\mu_{8,t}}-\underline{\mu_{8,t}}-\lambda^{\text{b}}=0,\quad s=\text{ref.bus},\forall t\in\Omega^t \quad (35)$$

$$\sum_s F^{\text{map}}_{l,s}\cdot\lambda_{1,t,s}+\lambda_{2,t,l}+\overline{\mu_{1,t,l}}-\underline{\mu_{1,t,l}}=0,\ \ \forall t\in\Omega^t,\forall l\in\Omega^l \quad (36)$$

$$-\sum_s W^{\text{map}}_{w,s}\cdot\lambda_{1,t,s}+\overline{\mu_{2,t,l}}-\underline{\mu_{2,t,l}}=0,\ \ \forall t\in\Omega^t,\forall w\in\Omega^w \quad (37)$$

$$-\sum_l F^{\text{map}}_{l,s}\cdot\lambda_{2,t,l}\cdot Y_l+\lambda_{3,t}=0,\ \ \forall t\in\Omega^t,\forall s\in\Omega^s \quad (38)$$

$$(-\overline{F_l}+f_{t,l})\cdot\overline{\mu_{1,t,l}}=0,\ \ \forall t\in\Omega^t,\forall l\in\Omega^l \quad (39)$$

$$(-\overline{F_l}-f_{t,l})\cdot\underline{\mu_{1,t,l}}=0,\ \ \forall t\in\Omega^t,\forall l\in\Omega^l \quad (40)$$

$$(w^{prod}_{t,w}-\overline{W_{t,w}})\cdot\overline{\mu_{2,t,w}}=0,\ \ \forall t\in\Omega^t,\forall w\in\Omega^w \quad (41)$$

$$-w^{prod}_{t,w}\cdot\underline{\mu_{2,t,w}}=0,\ \ \forall t\in\Omega^t,\forall w\in\Omega^w \quad (42)$$

$$(-\sum_b g_{t-1,i,b}+\sum_b g_{t,i,b}-RU_i)\cdot\mu_{3,t,i}=0,\ \ \forall t\in\Omega^t,\forall i\in\Omega^i \quad (43)$$

$$(\sum_b g_{t-1,i,b}-\sum_b g_{t,i,b}-RD_i)\cdot\mu_{4,t,i}=0,\ \ \forall t\in\Omega^t,\forall i\in\Omega^i \quad (44)$$

$$(-\lambda^{\text{g,i,b}}+g_{t,i,b})\cdot\overline{\mu_{5,t,i,b}}=0,\ \ \forall t\in\Omega^t,\forall i\in\Omega^i,\forall b\in\Omega^b \quad (45)$$

$$-g_{t,i,b}\cdot\underline{\mu_{5,t,i,b}}=0,\ \ \forall t\in\Omega^t,\forall i\in\Omega^i,\forall b\in\Omega^b \quad (46)$$

$$(p^{\text{ch}}_t-\overline{p^{\text{ch}}_t})\cdot\overline{\mu_{6,t}}=0,\ \ \forall t\in\Omega^t \quad (47)$$

$$-p^{\text{ch}}_t\cdot\underline{\mu_{6,t}}=0,\ \ \forall t\in\Omega^t \quad (48)$$

$$(p^{\text{dis}}_t-\overline{p^{\text{dis}}_t})\cdot\overline{\mu_{7,t}}=0,\ \ \forall t\in\Omega^t \quad (49)$$

$$-p^{\text{dis}}_t\cdot\underline{\mu_{7,t}}=0,\ \ \forall t\in\Omega^t \quad (50)$$

$$(p^{\text{h}}_t-\overline{p^{\text{h}}_t})\cdot\overline{\mu_{8,t}}=0,\ \ \forall t\in\Omega^t \quad (51)$$

$$-p^{\text{h}}_t\cdot\underline{\mu_{8,t}}=0,\ \ \forall t\in\Omega^t \quad (52)$$

$$\mu\geq 0,\ \ \forall k\in\Omega^k \quad (53)$$

REFERENCES

[1] M. Stecca, L. R. Elizondo, T. B. Soeiro, P. Bauer, and P. Palensky, "A comprehensive review of the integration of battery energy storage systems into distribution networks," *IEEE Open Journal of the Industrial Electronics Society*, vol. 1, pp. 46–65, 2020.

[2] M. Gržanić, T. Capuder, N. Zhang, and W. Huang, "Prosumers as active market participants: A systematic review of evolution of opportunities, models and challenges," *Renewable and Sustainable Energy Reviews*, vol. 154, p. 111859, 2022.

[3] *IRENA: Green hydrogen cost production*, IRENA. [Online]. Available: https://irena.org/-/media/Files/IRENA/Agency/Publication/2020/Dec/IRENA_Green_hydrogen_cost_2020.pdf

[4] *A hydrogen strategy for a climate-neutral Europe*, European Commision. [Online]. Available: https://ec.europa.eu/energy/sites/ener/files/hydrogen_strategy.pdf

[5] *A Hydrogen exchange for the Climate*, Government of the Netherlands. [Online]. Available: https://www.government.nl/documents/reports/2020/09/24/a-hydrogen-exchange-for-the-climate

[6] H. Pandžić and I. Kuzle, "Energy storage operation in the day-ahead electricity market," in *2015 12th International Conference on the European Energy Market (EEM)*. IEEE, 2015, pp. 1–6.

[7] K. Šepetanc and H. Pandžić, "A cluster-based operation model of aggregated battery swapping stations," *IEEE Transactions on Power Systems*, vol. 35, no. 1, pp. 249–260, 2019.

[8] E. Nasrolahpour, J. Kazempour, H. Zareipour, and W. D. Rosehart, "A bilevel model for participation of a storage system in energy and reserve markets," *IEEE Transactions on Sustainable Energy*, vol. 9, no. 2, pp. 582–598, 2017.

[9] A. Shahmohammadi, R. Sioshansi, A. J. Conejo, and S. Afsharnia, "Market equilibria and interactions between strategic generation, wind, and storage," *Applied Energy*, vol. 220, pp. 876–892, 2018.

[10] H. Mohsenian-Rad, "Coordinated price-maker operation of large energy storage units in nodal energy markets," *IEEE Transactions on Power Systems*, vol. 31, no. 1, pp. 786–797, 2015.

[11] Y. Ye, D. Papadaskalopoulos, and G. Strbac, "An mpec approach for analysing the impact of energy storage in imperfect electricity markets," in *2016 13th International Conference on the European Energy Market (EEM)*. IEEE, 2016, pp. 1–5.

[12] C. Wang, W. Wei, J. Wang, L. Wu, and Y. Liang, "Equilibrium of interdependent gas and electricity markets with marginal price based bilateral energy trading," *IEEE Transactions on Power Systems*, vol. 33, no. 5, pp. 4854–4867, 2018.

[13] T. Jiang, C. Yuan, L. Bai, B. H. Chowdhury, R. Zhang, and X. Li, "Bi-level strategic bidding model of gas-fired units in the interdependent electricity and natural gas markets," *IEEE Transactions on Sustainable Energy*, 2021.

[14] G. Pan, W. Gu, H. Qiu, Y. Lu, S. Zhou, and Z. Wu, "Bi-level mixed-integer planning for electricity-hydrogen integrated energy system considering levelized cost of hydrogen," *Applied Energy*, vol. 270, p. 115176, 2020.

[15] J. Huang, W. Li, X. Wu, and Z. Gu, "A bi-level capacity planning approach of combined hydropower hydrogen system," *Journal of Cleaner Production*, vol. 327, p. 129414, 2021.

[16] M. H. Shams, M. MansourLakouraj, J. J. Liu, M. S. Javadi, and J. P. Catalão, "Bi-level two-stage stochastic operation of hydrogen-based microgrids in a distribution system," in *2021 International Conference on Smart Energy Systems and Technologies (SEST)*. IEEE, 2021, pp. 1–6.

[17] V. H. Cantú, C. Azzaro-Pantel, and A. Ponsich, "A novel matheuristic based on bi-level optimization for the multi-objective design of hydrogen supply chains," *Computers & Chemical Engineering*, vol. 152, p. 107370, 2021.

[18] H. Pandžić and V. Bobanac, "An accurate charging model of battery energy storage," *IEEE Transactions on Power Systems*, vol. 34, no. 2, pp. 1416–1426, 2019.

[19] H. Pandžić, Y. Wang, T. Qiu, Y. Dvorkin, and D. S. Kirschen, "Near-optimal method for siting and sizing of distributed storage in a transmission network," *IEEE Transactions on Power Systems*, vol. 30, no. 5, pp. 2288–2300, 2014.

[20] *Study on early business cases for H2 in energy storage and more broadly power to H2 applications*, FCH. [Online]. Available: https://www.fch.europa.eu/sites/default/files/P2H_Full_Study_FCHJU.pdf